Improved Models for Long-Term Prediction of Tropospheric Scintillation on Slant Paths

Max M. J. L. van de Kamp, *Student Member, IEEE*, Jouni K. Tervonen, Erkki T. Salonen, and J. Pedro V. Poiares Baptista, *Member, IEEE*

***Abstract*—The prediction models for tropospheric scintillation on earth-satellite paths from Karasawa, Yamada, and Allnutt and ITU-R are compared with measurement results from satellite links in Europe, the United States, and Japan at frequencies from 7 to 30 GHz and elevation angles of 3 to 33°. The existing prediction models relate the long-term average scintillation intensity to the wet term of refractivity at ground level. The comparison shows that the seasonal variation of scintillation intensity is well predicted by this relation, but for the annual average some additional meteorological information is needed. A much better agreement with measurement results is found when a parameter representing the average water content of heavy clouds is incorporated. This confirms the assumption that scintillation is, at least partly, associated with turbulence inside clouds. The asymmetry between the distributions of signal fade and enhancement can also be explained by turbulence inside clouds. The asymmetry depends on the intensity of the scintillation, which is consistent with the theory assuming a thin layer of cloudy turbulence. A new model based on this theory predicts the distributions of signal fade and enhancement significantly better.**

***Index Terms*—Cloud water content, cumulus clouds, low-fade margin, meteorology, propagation, radio-wave propagation, satellite communication, tropospheric scintillation, tropospheric turbulence.**

I. Introduction

INCREASING demand for Ku-band (14/12/11 GHz) resources will require the provision of additional spectrum in higher bands. Some systems are already designed to operate in the 30/20 GHz band (Ka band) and it is probable that serious consideration will be given soon to utilizing the 50/40 GHz band (V band). Ka- and V-band applications will be aimed at very small aperture terminal (VSAT) services with low-fade margins. Thus, there is a pressing need to quantify attenuation phenomena in the relatively low-fade margin range. Furthermore, new satellite constellations using low earth orbits such as Teledesic and Iridium are planned with Ka-band links, which may have to operate occasionally at low elevation angles, where tropospheric scintillation may be a significant impairment.

Tropospheric scintillation is a rapid fluctuation of signal amplitude and phase due to turbulent irregularities in temperature, humidity, and pressure, which translate into small-scale variations in refractive index. In the microwave region, where the humidity fluctuations are important, the result is random degradation and enhancement in signal amplitude and phase received on a satellite–earth link, as well as a degradation in performance of large antennas.

In general, the impact of rain attenuation on communication signals is predominant at frequencies $\leq$10 GHz. Scintillation, however, becomes important for low-fade margin systems operating at frequencies $\geq$10 GHz and at low elevation angles ($\leq\approx 15°$) since on these, scintillation may cause as much attenuation as rain, especially for time percentages larger than 1%. Knowledge of the dynamic characteristics of scintillation is also important for the design of up-link power control and antenna tracking systems.

Early models for the prediction of scintillation effects relate the long-term scintillation intensity to the wet term of the refractivity at ground level, which is a function of temperature and humidity. When these models were formulated, few measurement results were available to verify the predictions. A number of new measurement results are now available, and the models are tested here using these results from several different sites in different continents.

II. Current Prediction Models

A. Long-Term Correlation with Meteorology

Karasawa *et al*. [1] presented a prediction method for the calculation of the standard deviation σ of signal fluctuations due to scintillation, based on measurements made during 1983 at Yamaguchi, Japan, at an elevation angle of 6.5°, frequencies of 11.5 and 14.23 GHz, and an antenna diameter of 7.6 m. For the elevation angle dependence, they used long-term data from the same site at elevation angles of 4° and 9°. Using these data, they derived the following prediction formula:

$$\sigma_{\text{pre}} = 0.0228(0.15 + 5.2 \times 10^{-3} N_{\text{wet}}) \cdot f^{0.45} \sqrt{G(D_e)} / \sin^{1.3} \varepsilon \quad \text{dB} \tag{1}$$

where

$$N_{\text{wet}} = \frac{22790 U e^{19.7t/(t+273)}}{(t+273)^2} \quad (\text{ppm}) \tag{2}$$

Manuscript received September 30, 1997; revised June 5, 1998. This work was supported in part by Helsinki University of Technology, Helsinki, Finland, under ESA/ESTEC Contract 10827/94/NL/NB(SC).

M. M. J. L. van de Kamp is with the Eindhoven University of Technology, Radiocommunications Group, 5600 MB Eindhoven, The Netherlands.

J. K. Tervonen is with the Helsinki University of Technology, Radio Laboratory, 02015 HUT, Helsinki, Finland.

E. T. Salonen is with the University of Oulu, Telecommunications Laboratory, 90571 Oulu, Finland.

J. P. V. Poiares Baptista is with the ESA/ESTEC, XEP, 2200 AG Noordwijk, The Netherlands.

Publisher Item Identifier S 0018-926X(99)03733-3.

and $\sigma_{\rm pre}$ is the predicted signal standard deviation or "scintillation intensity," f is the frequency in GHz, ε is the apparent elevation angle, $N_{\rm wet}$ is the wet term of the refractivity at ground level, U is the relative humidity in percent, and t is the temperature in degrees centigrade. These meteorological input parameters should be averaged over a period in the order of a month so the model does not predict short-term scintillation variations with daily weather changes. $G(D_e)$ is an antenna averaging function, given by Crane and Blood [2], and D_e is the effective antenna diameter given by $D_e = D\sqrt{\eta}$ with D as the geometrical antenna diameter and η the antenna aperture efficiency. The antenna averaging function also depends on the elevation angle and the height of the turbulence, assumed by Karasawa *et al.* to be 2000 m. If $\varepsilon < 5°$, $\sin\varepsilon$ in (1) should be replaced by $(\sin\varepsilon + \sqrt{\sin^2\varepsilon + 2h/R_e})/2$, where h is the height of the turbulence and R_e is the effective earth radius $= 8.5 \times 10^6$ m.

The Karasawa model was tested against measurements from four different sites in Western Japan and from Haystack, IA, and Chilbolton, U.K. These measurements were made at elevation angles from 4 to 30°, frequencies from 7.3 to 14.2 GHz, and with antenna diameters from 3 to 36.6 m. The average $N_{\rm wet}$ in these different databases varied from 20 to 130 ppm. Karasawa *et al.* mention that the model is expected to be applicable to worldwide regions with different meteorological conditions, but state that to verify or improve the prediction procedure, a collection of data at lower elevation angles and from different climatic regions is required.

ITU-R Recommendation PN 618-3 [3] contains another model, based upon measurements covering elevation angles in the range of 4–32°, antenna diameters between 3 and 36 m, a frequency range of 7–14 GHz, and several different climatic regions:

$$\sigma_{\rm pre} = (3.6 \times 10^{-3} + 10^{-4} N_{\rm wet}) f^{7/12} g(D_e) / \sin^{1.2}\varepsilon \quad \text{dB} \tag{3}$$

where $g(D_e)$ is the aperture averaging function from Haddon and Vilar [4]. A turbulent height of 1000 m is suggested by ITU-R. Also in this model, the meteorological parameters should be averaged over a period in the order of one month.

B. Signal-Level Distribution

Karasawa *et al.* [1] also present some expressions for the long-term cumulative distribution of amplitude deviation y, expressed in terms of the predicted long-term standard deviation. They derived this expression theoretically, using the integration formula

$$p(y) = \int_0^\infty p(\sigma) p(y|\sigma)\, d\sigma \tag{4}$$

where $p(\sigma)$ is the distribution function of short-term standard deviations for which Karasawa *et al.* assume a Gamma distribution and $p(y|\sigma)$ is the conditional short-term distribution function of signal level y for a given standard deviation σ, which is generally assumed to be a Gaussian distribution. The resulting amplitude deviation, exceeded for a time percentage of P is given by

$$y = (-0.0597 \log^3 P - 0.0835 \log^2 P - 1.258 \log P + 2.672)\sigma_{lt} \qquad (0.01\% \le P \le 50\%) \tag{5}$$

where σ_{lt} is the long-term signal standard deviation, which can be calculated from (1). Equation (5) agreed well with the measurements of Karasawa *et al.* for signal enhancement. For signal fade, however, the measured deviation was larger, especially in the low probability region. They fitted a curve to these measurement results, giving the relation

$$y = (-0.061 \log^3 P + 0.072 \log^2 P - 1.71 \log P + 3.0)\sigma_{lt} \qquad (0.01\% \le P \le 50\%). \tag{6}$$

The difference between fade and enhancement is due to an asymmetry in the short-term signal-level fluctuations, which is especially evident for strong scintillations.

The ITU-R [3] adopted only the distribution (6) for signal fade in their proposed prediction method.

III. Comparison and Analysis

A. Long-Term Correlation with Meteorology

The prediction models of long-term scintillation intensity [(1) and (3)] from ITU-R and Karasawa *et al.* have been compared to the new measurement results from Kirkkonummi, Finland, at 19.77 and 29.66 GHz by van de Kamp *et al.* [5]. It appeared that both of the models predicted a higher intensity than that measured at Kirkkonummi—the Karasawa model being the closer one. Similar comparisons with measured data have been made also at other sites, (e.g., [6], [7]), and similar discrepancies were found. However, the prediction models should not be redefined on the basis of the measurement results at one site only. A globally applicable model to predict signal impairments due to tropospheric scintillation will have to be validated with global data as Karasawa *et al.* suggested. Such an extensive database is not yet available. Nevertheless, in this paper a further step is taken toward a global prediction model, using measurement results found available in literature.

1) Comparison of Global Measurement Results with the Models: For this analysis, measurement results of long-term scintillation intensity, measured over at least several months, have been extracted from literature. In order to compare also the seasonal correlation of scintillation and meteorological parameters, results were used which were presented with a time resolution of three months or shorter. No time resolution shorter than one month is considered. This is partly because the existing prediction models were proposed for this time resolution and partly because most of the results are presented with this time resolution. However, it should be noted that a significant correlation between scintillation intensity and $N_{\rm wet}$ can also be found on a shorter time base [5].

A collection of measured data from 12 sites in three continents was found [1], [5]–[16]. These published results are usually presented in graphs. The data have been extracted from these by enlarging the paper copies. This way, an estimated accuracy of ≈0.1% of the maximum range of the graphs could be reached.

TABLE I
SITE PARAMETERS: STATION NAMES, GEOGRAPHICAL COORDINATES (LATITUDE AND LONGITUDE), FREQUENCIES f, ELEVATION ANGLES ε, ANTENNA DIAMETERS D, APERTURE EFFICIENCIES η, SATELLITE NAMES, AND SECTIONS OF THIS PAPER WHERE THE RESULTS ARE USED. IF η IS NOT INDICATED, IT IS NOT GIVEN IN THE REFERENCE

Site	coordinates (N - E)	f (GHz)	ε (°)	D (m)	η ( )	Satellite	Section (III-)
Austin [7]	30.39 - 262.27	11.20	5.8	2.4		Intelsat-510/602	A, B
Chilbolton [21]	51.07 - 358.68	11.20	7.1	3		Intelsat-V	B
Darmstadt [8]	49.87 - 8.63	12.50	27	1.8	0.5	Olympus	A
		19.77		3.7	0.5		A
		29.66		3.7	0.5		A
Eindhoven [9]	51.45 - 5.49	12.50	26.8	5.5	0.92	Olympus	A
		19.77			0.78		A
		29.66			0.44		A
Fairbanks [10]	64.86 - 212.18	20.19	7.92	1.22	0.56	ACTS	A, B
		27.51					A
Goonhilly [6], [22]	50.05 - 354.83	11.20	3.27	1.44	0.65	Intelsat-507	A, B
Haystack [1], [11]	42.34 - 288.74	7.3	5	36.6			A
Kirkkonummi [5]	60.22 - 24.40	19.77	12.7	1.8	0.63	Olympus	A, B
		29.66			0.38		A, B
Leeheim [12], [14]	49.51 - 8.30	11.79	32.9	3		OTS-II	A, B
				8.5			A
Martlesham [15]	52.06 - 1.29	≈11	≈10	6.1	0.62	Intelsat-V	A
Ohita [1]	33.25 - 131.60	11.45	6.6	4		Intelsat-V	A
Okinawa [1]	26.50 - 128.00	11.45	11.3	4		Intelsat-V	A
Portsmouth [23]	50.79 - 358.91	11.79	30.9	2.4	0.55	OTS-II	B
Yamaguchi [1], [16]	34.18 - 131.55	11.45	6.5	7.6		Intelsat-V	A, B

The site parameters relevant for further analysis are summarized in Table I. Some details on the data processing procedures at the different measurement sites are given in Appendix A.

Due to the different frequency and geometrical configuration of each measurement setup, it is necessary to use a normalized scintillation intensity to be able to perform a useful comparison. Assuming the dependence on frequency, elevation angle, and antenna size as described in the models of ITU-R and Karasawa, a normalized scintillation intensity σ_n can be defined as

$$\sigma_n = \frac{\sigma}{f^a g(D_e)/\sin^b \varepsilon} \tag{7}$$

where $a = 0.45$ and $b = 1.3$ according to Karasawa and $a = 7/12$ and $b = 1.2$ according to ITU-R. $g(D_e)$ is the antenna averaging function of Haddon and Vilar. According to both models, σ_n should be only dependent on N_{wet}. σ_n has been plotted versus the months of the year in Fig. 1, for all of the measurement sites. The coefficients a and b have, arbitrarily at this point, been chosen according to the model from Karasawa. The height of the turbulence has been assumed 2000 m and an antenna aperture efficiency of 0.75 has been assumed if it was not indicated in the references.

For a comparison with the prediction models, meteorological data are also needed. Unfortunately, from Martlesham Heath [15], no meteorological measurements are reported. However, an extensive global meteorological database has been purchased by Helsinki University of Technology under contract to ESA from the European Centre for Medium-Range Weather Forecasts (ECMWF). This database contains height profiles of pressure, temperature, and absolute humidity on 23 height levels, for grid points over the whole earth with a resolution of 1.5° both in latitude and longitude and for every six hours in the period from October 1992 to September 1994. It was obtained by a combination of various measurements and model-based predictions.

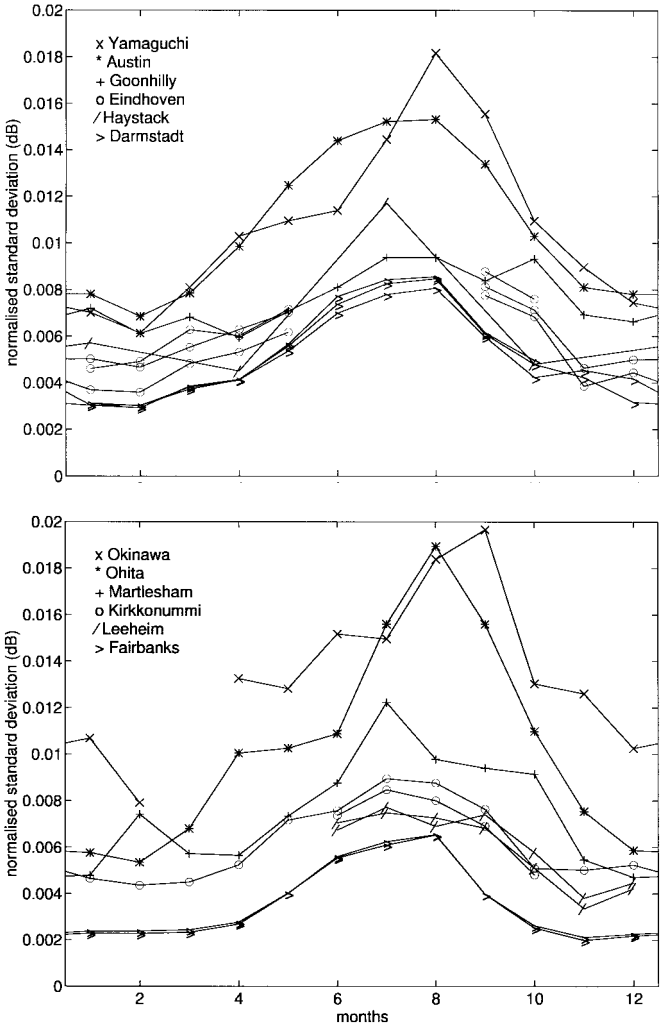

Fig. 1. Normalized scintillation intensity as a function of the months of the year for all of the considered measurement sites. Coefficients a and b in (7) according to Karasawa. The separation into two graphs is simply for a clearer view.

Although the time period of these data does not cover exactly the measured period in Martlesham, it still can be expected that on average the seasonal dependence of meteorological parameters does not change much over a few years so the data may still be representative for the measured period. This has been verified by comparing the monthly averaged N_{wet} obtained from the other sites where temperature and humidity were measured to the monthly averaged N_{wet} resulting from the ECMWF data set for the same places on earth. The root mean square (rms) error of the values from ECMWF with respect to the measured values was 8.8 ppm; the rms relative error was 15.9%. The impact of this error on the prediction of σ_n was evaluated by calculating the difference between the monthly values of σ_n predicted by the Karasawa model using the measured values of N_{wet} and those using the N_{wet} values from ECMWF. The rms absolute difference was 0.000 97 dB; the rms relative difference was 9.0%. It is,

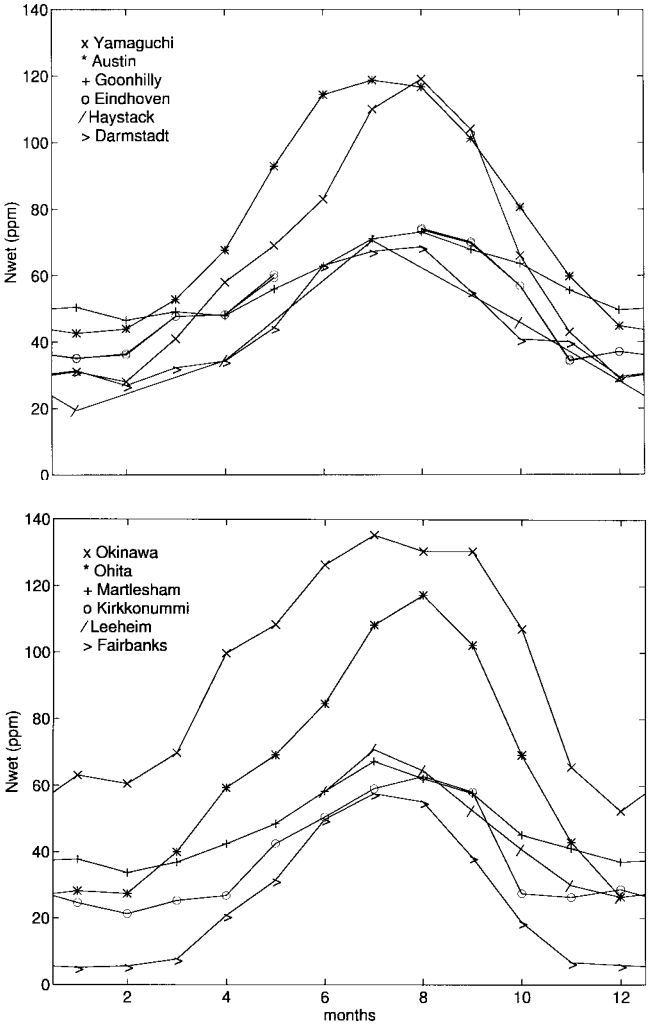

Fig. 2. Monthly averaged $N_{\rm wet}$ at all the sites, all from meteorological measurements, except those in Martlesham, which are from ECMWF.

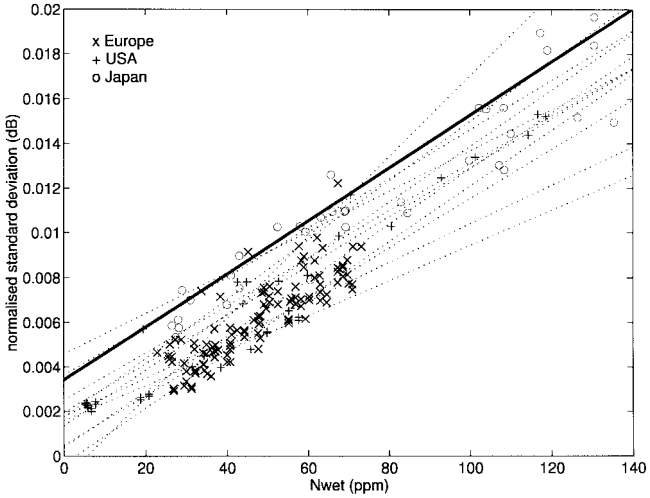

Fig. 3. Normalized scintillation intensity versus $N_{\rm wet}$ for all of the different sites, months, and frequencies. Theoretical relation from Karasawa (thick line) and individual linefits for the data from each site (dotted lines).

TABLE II
COMPARISON OF THE EXISTING AND PROPOSED NEW PREDICTION MODELS: CORRELATION COEFFICIENT OF $N_{\rm wet}$ VERSUS σ_n FOR KARASAWA AND ITU-R MODEL, AND OF $N_{wet} + Q$ VERSUS σ_n FOR THE NEW MODELS FOR ALL MEASUREMENT POINTS (MONTHLY AVERAGES), AND RMS RELATIVE ERROR OF THE MODEL-PREDICTED σ_n WITH RESPECT TO THE MEASURED σ_n FOR ALL MEASUREMENT POINTS (MONTHLY AVERAGES)

model	corr. coef.	rms. rel. error
Karasawa	0.931	58.3%
ITU-R	0.895	89.2%
using $W_{\rm hc}$	0.962	15.5%
using $P_{\rm hc}$	0.953	18.7%
using Cu	0.954	17.4%

therefore, expected that the ECMWF data can reasonably be used to estimate the monthly averaged $N_{\rm wet}$ of a site from which no meteorological results have been reported. Fig. 2 shows the monthly averaged $N_{\rm wet}$ as a function of the months, all from the measurements at the sites, except for those from Martlesham, which have been calculated from ECMWF data.

Fig. 3 shows a scatterplot of the normalized intensity σ_n (Fig. 1) versus $N_{\rm wet}$ (Fig. 2) for all sites, months, and frequencies. The theoretical relation according to Karasawa is also shown, as well as lines fitted to the data from each site separately. The correlation of all these results together is significantly worse than that of the results of each station separately, as can be expected. Furthermore, the gradients of the fitted lines for the separate stations are in general in good agreement with the model, but there is a considerably variable negative offset. In general, the offset is smallest in Japan (where the model came from) and largest in Europe. It can be concluded that Karasawa's model predicts the seasonal variation of the monthly average σ_n well for various places on earth, but not the annual average σ_n.

On the first line of Table II, the correlation coefficient of all points of Fig. 3 together is shown, as well as the rms relative error in σ made by the Karasawa model. The same calculations have been made using the model parameters a and b in (7) according to ITU-R, the result of which is also shown in Table II. This result appears to be even worse than that from Karasawa.

The fact that the situation does not improve by changing the frequency exponent a can be explained considering that at most of the stations, measurements were made at a frequency between 11 and 12.5 GHz. The relative positions of these measurement results are hardly affected by adjusting the frequency dependent term. The same thing can be said for the elevation angle dependent term, because different sites with similar elevation angles gave different results. Therefore, another way of improving the situation is considered in this paper. Further analysis is made starting from Karasawa's model configuration, since it gave the best result. An additional parameter for this model is sought.

2) Improvement Using Cloud Information: It has been observed several times that there is a significant correlation between the occurrence of scintillation and the presence of cumulus clouds along the propagation path. This gives the impression that at least part of the turbulent activity causing scintillation is associated with cumulus clouds. As an example, Mohd Yusoff *et al.* [6] found a significant difference in average

scintillation intensity for their "dry" and "wet" databases from Goonhilly and suggested that scintillation in the latter may be caused by turbulent mixing of air masses with different water contents in and around clouds and precipitation. They called this effect "turbulent attenuation." The parameter $N_{\rm wet}$ at ground level is not a good indicator of this kind of turbulence. Tervonen *et al.* [17] showed that the average variation of scintillation intensity over the hours of the day is uncorrelated with $N_{\rm wet}$ and strongly correlated with the cumulus cloud cover. Therefore, a new parameter indicating the average water content of "turbulent clouds" occurring on the propagation path may help to improve the prediction models of scintillation.

The ECMWF database provides a possibility to derive a parameter indicating the water content of turbulent clouds. Using the Salonen/Uppala cloud model (an improved version of the model first published in [18] and [19]), the occurrence, height, and thickness of clouds, as well as their water content as a function of height, can be calculated from the height profiles of pressure, temperature and humidity. This has been done for all the considered measurement sites, yielding for each site a time series of height profiles of the cloud water content. From this information various statistical cloud properties can be calculated.

For each site, we calculated the average water content of heavy clouds W_{hc}. Here, "heavy clouds" means a cloud layer with an integrated water content larger than 0.70 kg/m^2. W_{hc} indicates the integrated water content (including ice) of heavy clouds averaged over only the time during which these occurred. On average this parameter shows a climatic correlation with σ_n, which, in some cases, is better than that of $N_{\rm wet}$; e.g., the annual average W_{hc} in Darmstadt is lower than that in Kirkkonummi and Eindhoven as is the average σ_n, while the average $N_{\rm wet}$ is not. A climatic correlation of a long-term averaged parameter was exactly what was needed to improve the prediction models. W_{hc} has been incorporated in a new prediction model for σ_n in the following way:

$$\sigma_n = 0.98 \times 10^{-4}(N_{\rm wet} + Q) \tag{8}$$

$$Q = -39.2 + 56\overline{W}_{hc} \tag{9}$$

where the overscore denotes long-term (at least annual) average and W_{hc} is expressed in kg/m^2. In (8), Q is a long-term average parameter and, therefore, constant for each site so that all seasonal dependence of σ_n is still represented by $N_{\rm wet}$. The coefficients in (9) have been empirically adjusted to give maximum correlation between $(N_{\rm wet}+Q)$ and σ_n. The significant improvement in climatic correlation is illustrated by the correlation coefficients of annual averages: The correlation coefficient of annual average σ_n versus $N_{\rm wet}$ for all sites and frequencies is 0.943; that of σ_n versus $(N_{\rm wet} + Q)$ is 0.983.

A scatterplot of the monthly $N_{\rm wet} + Q$ versus σ_n for all the sites is shown in Fig. 4. The correlation coefficient of the points and the rms relative error of the new model are included in Table II. It is evident from both Fig. 4 and Table II that the performance of this model is considerably better than that of the Karasawa model for the data tested.

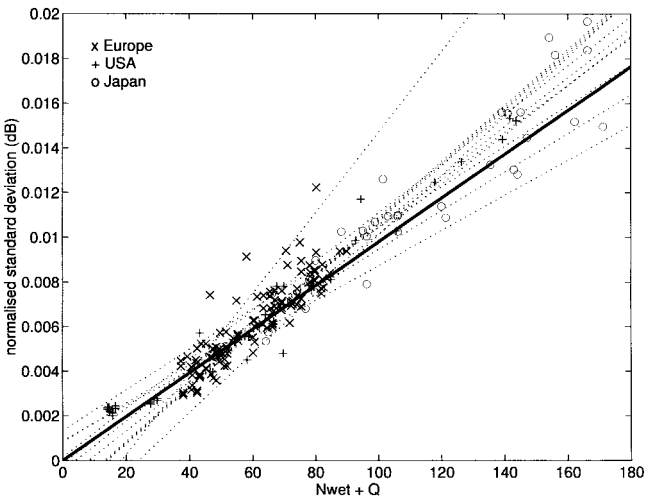

Fig. 4. σ_n versus $N_{\rm wet} + Q$ for all of the different sites, months, and frequencies. Individual line fits for the data from each site (dotted lines) and the new proposed model (thick line).

The outliers in Fig. 4 are data points from Martlesham, which is very likely due to the fact that the meteorological data for this site come from the ECMWF data set so that the monthly correlation between $N_{\rm wet}$ and σ_n is less good than that for the other sites. To illustrate this: it was checked that, if all $N_{\rm wet}$ values were taken from the ECMWF data instead of from the measurements, the overall spread in Fig. 4 would slightly increase and the Martlesham data would not be outliers anymore.

The performance of the new model is better even for the data from Yamaguchi, Ohita, Okinawa, and Haystack, on which Karasawa *et al.* had already tested their model [1]: for this data subset, the correlation coefficient of the monthly σ_n versus $(N_{\rm wet}+Q)$ is 0.943 and the rms relative error of the new model is 14.2%, while using the Karasawa model these figures are 0.937 and 22.1%.

Equations (7)–(9) together now form a new empirical model for the prediction of monthly averaged scintillation intensity. However, much more data from more different sites, in different climates and operating at different elevation angles and frequencies will have to be collected in order to validate this model and develop a globally applicable prediction model. It shows nevertheless from the above that scintillation is, at least partly, associated with turbulence in heavy clouds, and that the water content of heavy clouds W_{hc} (water content >0.70 kg/m^2) is a significant indicator of the annual average scintillation intensity, and is therefore a useful parameter to be combined with $N_{\rm wet}$, in order to improve the long-term performance of global scintillation prediction models.

In order to make a comparison with other measurement results possible, a global map of the long-term average water content of heavy clouds W_{hc} has been calculated from the ECMWF data. The result of this is shown in Fig. 5.

The same analysis as above has been performed with the "average probability of heavy clouds" P_{hc} as an extra parameter, indicating the probability of occurrence of the clouds with water content >0.70 kg/m^2. This parameter can also be calculated from the ECMWF data. A third alternative

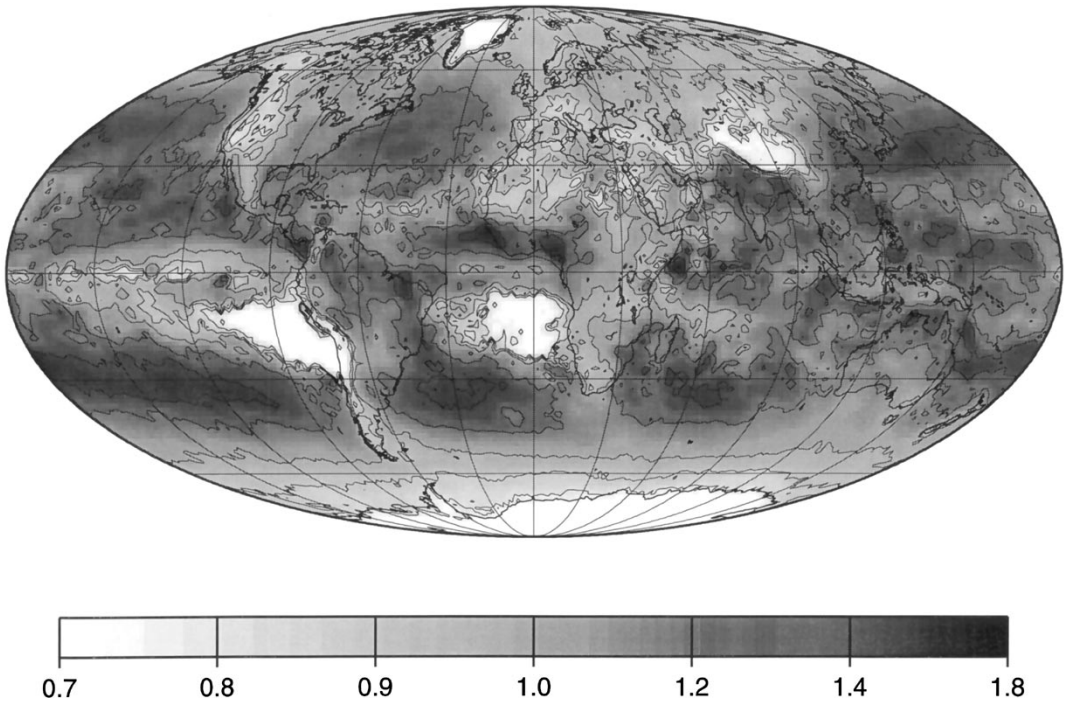

Fig. 5. Global map of the average water content of heavy clouds W_{hc} (indicated in kg/m^2).

parameter was found using the cumulus cloud amount. This parameter was obtained from the NDP026B public database of Carbon Dioxide Information Analysis Center (CDIAC) and National Center for Atmospheric Research (NCAR) [20]. This database consists of edited synoptic cloud reports from ships and land stations over the entire globe over the period from December 1981 to November 1991. The parameter "cumulus cloud amount" Cu indicates the portion of the sky covered with low level clouds, which are mainly cumulus clouds. This parameter has proved to be correlated with the variation of scintillation intensity over the hours of the day [17].

These analyses resulted in expressions similar to (8) and (9). The performances of these alternative models are included in Table II. As can be seen from this table, the performance of these alternatives is also considerably better than that of the Karasawa model and almost as good as the model using W_{hc}.

TABLE III
AVERAGE STANDARD DEVIATIONS OF THE SIGNALS IN THE ANALYZED DATA SETS

site	σ (dB)
Austin	0.62
Chilbolton	0.466
Fairbanks	0.24
Goonhilly	1.00
Kirkkonummi 20 GHz	0.165
Kirkkonummi 30 GHz	0.228
Leeheim	0.067
Portsmouth	0.086
Yamaguchi	0.54

B. Signal-Level Distribution

In this section, the prediction formulas of Karasawa *et al.* for the relation between the average standard deviation and the enhancement/fade distribution [(5) and (6)] are compared with measurement results from various sites.

1) Comparison of Global Measurement Results with the Models: For this analysis, results for the probability distribution of signal-level fluctuation from the mean have been extracted from publications, in a similar way to the previous section. Since in the prediction models, the fade and enhancement distributions are predicted from the long-term standard deviation σ_{lt}, only those sites which also report the average standard deviation measured over the same period have been selected.

Measurement results from eight sites in three continents were found [1], [7], [10], [14], [21]–[23]. The site parameters are summarized in Table I. The standard deviations of the signals in the reported data sets are listed in Table III. Some details on the data processing procedures at the different measurement sites are given in Appendix A.

In Fig. 6, the cumulative distributions for signal fade, and in Fig. 7, for signal enhancement are shown for all the measurement sites. All distributions have been divided by the respective standard deviations σ_{lt}, so that according to Karasawa *et al.*, they should all correspond to the model indicated in the figures (thick line). It is evident that this is not really the case. Especially the Goonhilly fade curve is far away from the others. The statement that those data "include rain effects as well" is probably meant as an explanation for the large discrepancy between the fade curve and the Karasawa model. This may be true, since they had difficulties in establishing a mean signal level [22], but because scintillation was almost all the time much more strongly present in the signal than

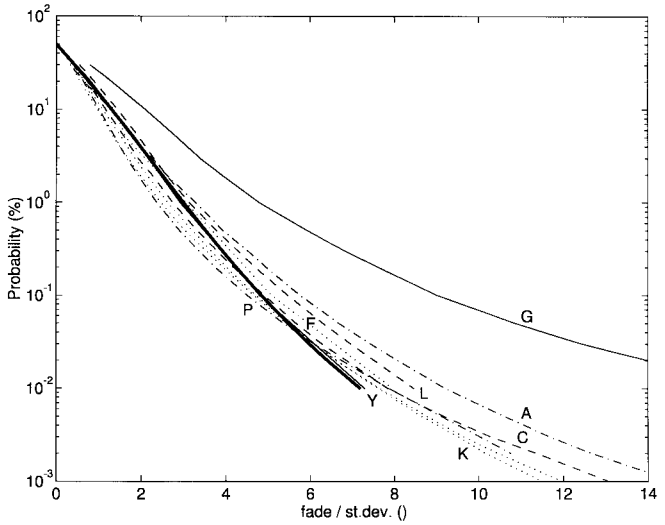

Fig. 6. Cumulative distributions of signal fade normalized by the standard deviations for all of the measurement sites and the model by Karasawa (thick line). The letters are initials of the names of the sites (see Table I or III for the full names).

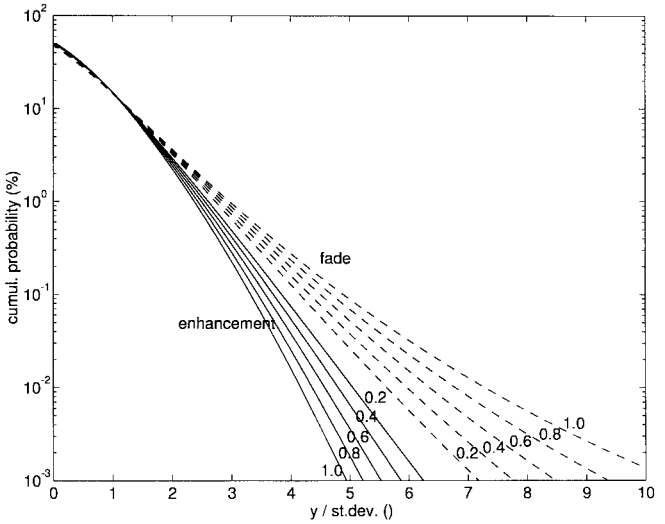

Fig. 8. Theoretical distribution of normalized signal enhancement and fade for the indicated values of the long-term standard deviation, assuming a Rice–Nakagami distribution for the short-term received electric field amplitude [24].

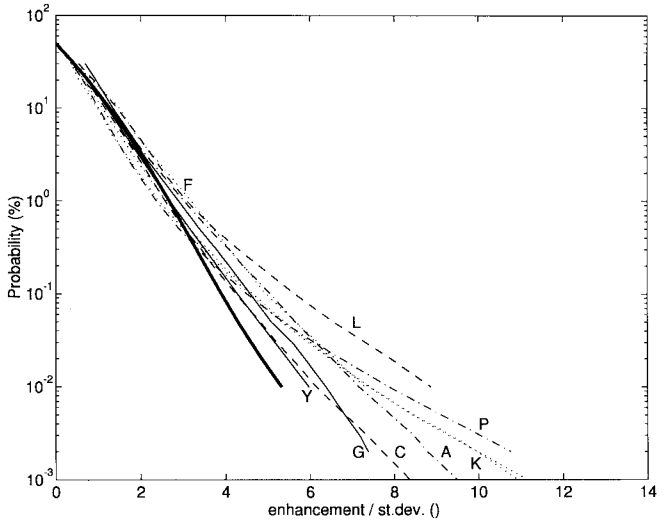

Fig. 7. Cumulative distributions of signal enhancement, normalized by the standard deviations for all of the measurement sites and the model by Karasawa (thick line).

rain attenuation, it should be expected that rain was not the only cause of this discrepancy. Another effect that is likely to play a role in the results for Goonhilly is multipath fading due to the layered structure of the troposphere. This effect, which is mostly observed on line-of-sight links, can also become significant on earth-space links with elevation angles below about 4° [3].

Since, however, also the other measurement results in Figs. 6 and 7 show significant deviations from the Karasawa model, it is expected that the Goonhilly results are a combination of scintillation and multipath fading. In general, the observations suggest that the fade and enhancement distributions normalized by the standard deviations are not as constant as suggested by Karasawa *et al.* In the next subsection, we will look for a physical model which explains the observed variations of the normalized signal distributions.

2) Improvement: The Karasawa model for signal enhancement had been derived assuming a Gaussian short-term distribution of signal level y in decibels. Van de Kamp [24] demonstrated that this assumption is not necessarily correct. As discussed in Section III-A, the main cause of scintillation on a satellite link is turbulence in clouds. This implies that the turbulent layer is likely to be a thin layer far from the receiver. From this modeling approach, it follows that the received electric field amplitude is on a short term Rice–Nakagami distributed and the distribution of signal level y in decibels is asymmetrical [24]. This can explain the difference between measured fade and enhancement. The effect of this on the long-term distribution of y is shown in Fig. 8; the normalized fade increases with the long-term standard deviation, while the normalized enhancement decreases. This agrees with the behavior observed in Figs. 6 and 7, which confirms the assumption of the thin turbulent layer and the Rice–Nakagami distribution.

The results of Figs. 6 and 7 do not quantitatively exactly match with the theoretical results of Fig. 8. This can be due to the assumption of the long-term gamma distribution of the short-term standard deviation σ, with $m_\sigma^2 = 10\sigma_\sigma^2$, where m_σ is the long-term mean of σ, generally equal to long-term standard deviation σ_{lt}, and σ_σ is the long-term standard deviation of σ. This relation was stated by Karasawa *et al.* [1] and also used in the derivation of Fig. 8. If, however, e.g., σ_σ is in reality larger with respect to m_σ than assumed, the spread of the gamma distribution will be larger and strong short-term fluctuations will occur more frequently for the same long-term mean standard deviation, resulting in larger normalized fades and enhancements exceeded for small probabilities.

It could now be suggested to look for a globally applicable relation between m_σ and σ_σ. However, for this, the best way would be to compare measured values of m_σ and σ_σ from different sites, but these are not available. Instead, we will look for a model that expresses the distributions of normalized fade and enhancement qualitatively similar to Fig. 8. Let us

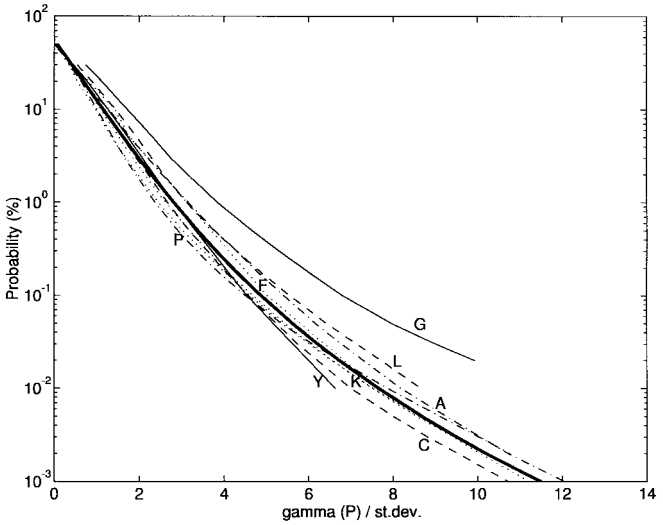

Fig. 9. The function $\gamma(P)/\sigma_{lt}$ for all of the different measurement sites and a new proposed model curve (thick line).

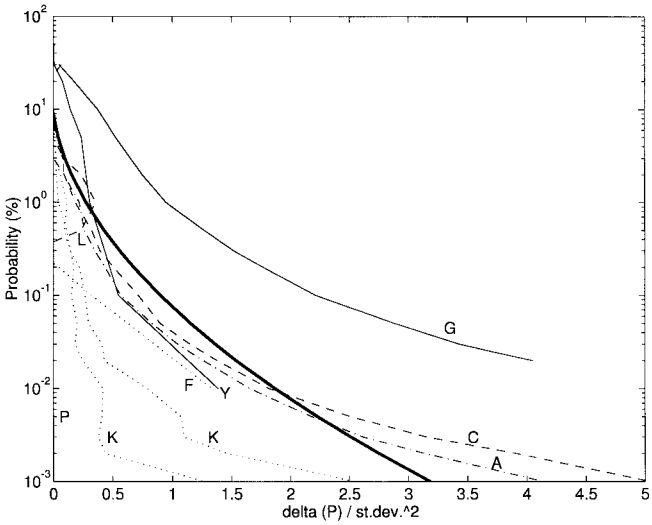

Fig. 10. The function $\delta(P)/\sigma_{lt}^2$ for all of the different measurement sites and a new proposed model curve (thick line).

first define

$$\gamma(P) = (y_f(P) + y_e(P))/2$$
$$\delta(P) = (y_f(P) - y_e(P))/2 \tag{10}$$

where

$y_f(P)$ the distribution of signal fade (decibels);
$y_e(P)$ the distribution of signal enhancement (decibels).

In Fig. 9, $\gamma(P)$ is shown normalized by dividing it by σ_{lt} for all the measurement sites. This corresponds to the average of normalized fade and enhancement in Fig. 8, which is approximately independent of σ_{lt} there. In Fig. 9, the results are indeed similar for all sites except Goonhilly. A curve has been fitted to these results and is indicated in the graph (thick line).

The difference between normalized fade and enhancement is approximately proportional to σ_{lt} in Fig. 8, so $\delta(P)$ is approximately proportional to σ_{lt}^2. In Fig. 10, $\delta(P)$ has been plotted for all sites, divided by σ_{lt}^2. Here it is seen that the results from the different sites almost converge. In Fairbanks, Kirkkonummi, Leeheim, and Portsmouth both $\delta(P)$ and σ_{lt}^2 are too small for an accurate calculation. A curve has been fitted to the results of Austin, Chilbolton, and Yamaguchi, and indicated in the graph (thick line). The fitted curves give the following expressions:

$$\gamma(P) = (-0.0515 \log^3 P + 0.206 \log^2 P - 1.81 \log P + 2.81)\sigma_{lt} \tag{11}$$
$$\delta(P) = (0.172 \log^2 P - 0.454 \log P + 0.274)\sigma_{lt}^2 \tag{12}$$

where σ_{lt} = long-term standard deviation (decibels).

Equations (10)–(12) now form a new model for the long-term distribution of signal level. The advantages of this model with respect to Karasawa's model are that the asymmetry of the long-term distribution is now theoretically predicted and this asymmetry increases with the scintillation intensity, consistently with measurement results.

The performance of this new model is compared with that of Karasawa's model in Table IV where the rms absolute and relative deviations from all of the measured distributions are compared. The probability range between 20 and 50% is not considered because the absolute error is small anyway and the relative error may become unreasonably large. In this table, the improvement with respect to the Karasawa model is evident, especially considering that for the Karasawa model the probability range between 0.01 and 0.001% was not considered since the model is not defined there. The new model performs less good than the Karasawa model only in Yamaguchi, which is for the measurements on which the Karasawa model was based. In Chilbolton, the absolute error of the new model is slightly larger due to values at very low probability levels. For all other sites the new model shows a significant improvement with respect to the Karasawa model. The improvement also shows clearly in Fig. 11, where the models are plotted together with the measured distributions for some of the sites.

In Goonhilly, there is still a significant difference between the measured fading and the new model, which can be ascribed to multipath fading due to the layered structure of the atmosphere, as discussed before. It can, therefore, be expected that the new model describes turbulence induced scintillation,

TABLE IV
EVALUATION OF NEW MODEL OF SIGNAL FADE AND ENHANCEMENT DISTRIBUTION: ABSOLUTE AND RELATIVE RMS ERRORS OF NEW MODEL OVER THE RANGE $0.001\% \le P \le 20\%$ AND THE KARASAWA MODEL, OVER THE RANGE $0.01\% \le P \le 20\%$. "TOTAL" INDICATES THE RMS ERROR OF ALL RESULTS TOGETHER EXCEPT THOSE FROM GOONHILLY

	abs. errors (dB)		rel. errors (%)	
measurements from:	Karasawa model	new model	Karasawa model	new model
Austin	0.60	0.30	16.3	9.3
Chilbolton	0.16	0.23	8.2	7.5
Fairbanks	0.22	0.07	15.5	10.9
Goonhilly	2.63	1.96	31.2	27.5
Kirkkonummi 20 GHz	0.11	0.04	21.6	12.1
Kirkkonummi 30 GHz	0.15	0.07	14.3	5.8
Leeheim	0.09	0.04	19.5	14.0
Portsmouth	0.07	0.03	20.4	12.0
Yamaguchi	0.19	0.38	8.7	12.1
total	0.25	0.19	16.3	10.8

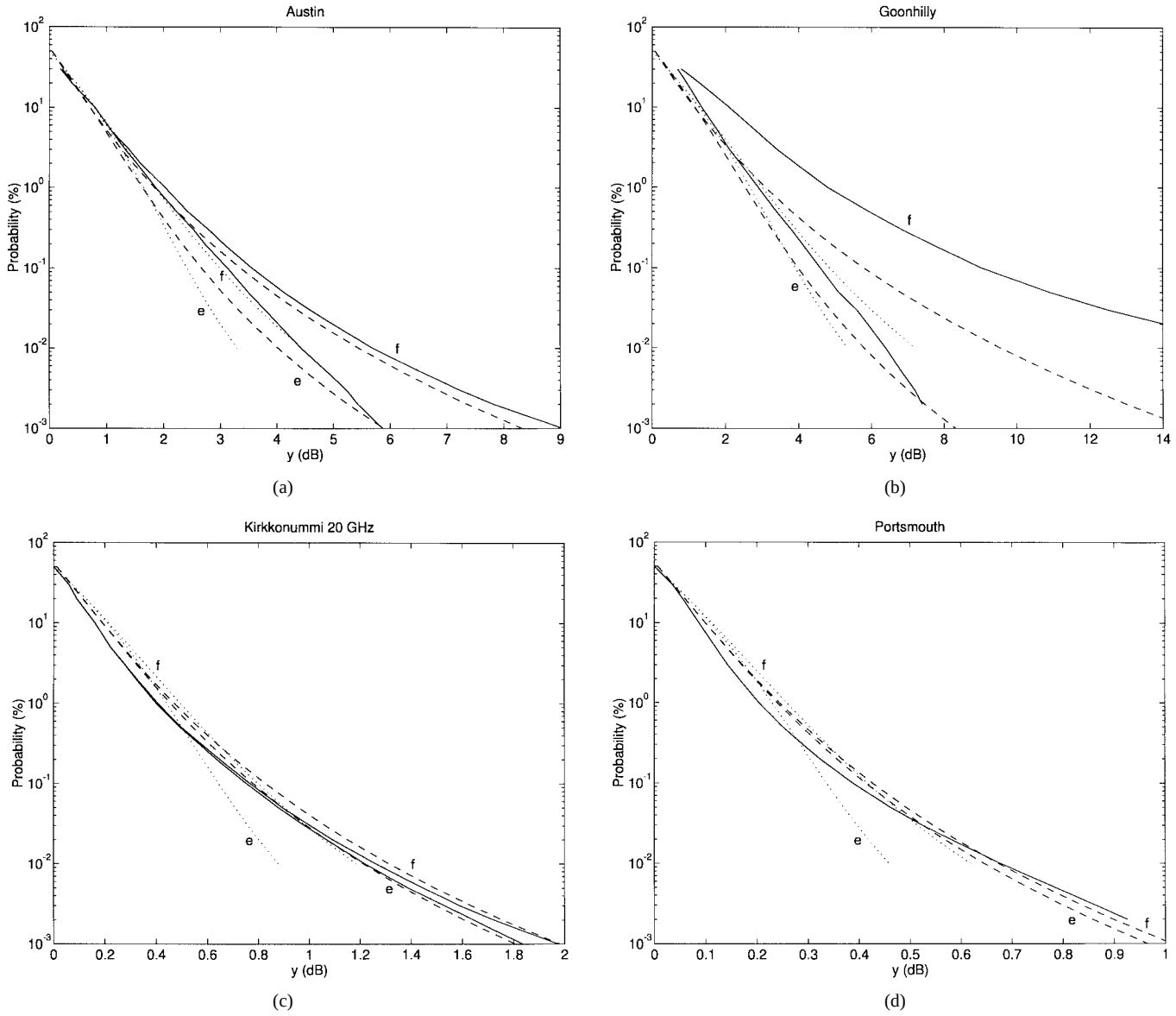

Fig. 11. Measured and modeled distributions of fade and enhancement in (a) Austin, (b) Goonhilly, (c) Kirkkonummi (19.77 GHz), and (d) Portsmouth: — — — measured distribution, - - - - - new proposed model, and · · · · · Karasawa model. "f" = fade; "e" = enhancement.

which dominates the clear weather signal fluctuations for elevation angles above about 4°. For lower elevation angles, another asymmetric component describing multipath fading should be added.

IV. Conclusions

It is found from a comparison of the current scintillation prediction models with available global data that N_{wet} is not sufficient as a single meteorological input for long-term scintillation intensity prediction. There are significant indications that at least part of the measured scintillation is caused by turbulence in clouds. The water content of heavy clouds W_{hc} (water content $>$ 70 kg/m^2) provides a good parameter to represent the scintillation due to cloudy turbulence. A new scintillation prediction model using both N_{wet} and W_{hc} shows a significantly better performance than the current models. As alternatives to W_{hc}, the average probability of heavy clouds or the cumulus cloud amount may also be used.

The normalized (i.e., divided by long-term standard deviation) distributions of signal fade and enhancement have significantly varying shapes at various sites. This is not predicted by the Karasawa model. The theory assuming a thin turbulent layer and a Rice–Nakagami distribution for the short-term variations of electric field amplitude not only predicts the asymmetry of the long-term signal-level distribution (in contrast to the theory of Karasawa's model), but also predicts a dependence of this asymmetry on the long-term standard deviation, similar to the dependence observed. A new model that takes this dependence into account can predict the long-term distribution of signal level significantly better. At elevation angles below about 4°, multipath fading also contributes to the measured signal fluctuations, increasing the asymmetry further.

Furthermore, it is reiterated that the development of global prediction models of both the long-term scintillation intensity and the signal-level distribution still requires much more data from measurement sites in different climates, and operating at

different frequencies and elevation angles, so the new models can be validated and improved further. The use of large global databases, as done in this paper, is essential for the development of semi-empirical models as the ones discussed here for which the physical relations are qualitatively known to some extent but need be quantified experimentally.

At this juncture, it is proposed that the prediction models presented in this paper, of the long-term scintillation intensity and the long-term signal-level distribution due to scintillation, be used in the design of satellite links. For the model of the long-term intensity, global maps of the necessary meteorological information are available, generated from the ECMWF database. The information can be obtained by contacting the authors of this paper.

Appendix A
Details on the Data Processing Procedures at the Different Measurement Sites

After each description is indicated in which section of this paper the results are used.

Austin, TX [7]: The University of Texas reported measurements under contract with INTELSAT covering the period June 1988 to May 1992, during which the right-hand circularly polarized 11.20 GHz signal from a succession of three geostationary satellites in the same orbital location was monitored. The receiver output was sampled at 2 Hz and the meteorological sensors of temperature and humidity at 0.1 Hz. Slowly varying signal components were removed by subtracting the signal averaged over consecutive 6-min intervals. The standard deviation calculated over every hour is reported averaged over every day and $N_{\rm wet}$ averaged over approximately a two week period. We have averaged these results over each month (Section III-A). In addition, the signal fluctuation statistics were derived from June 1988 to May 1991. The resulting distributions have been submitted to the databank "DBSG5" of ITU-R [13] (Section III-B).

Chilbolton, U.K. [21]: A satellite beacon receiving station has been in operation at the U.K. SERC Chilbolton Observatory between July 1983 and September 1984. The received signal was the 11.20 GHz beacon from an INTELSAT-V satellite over the Indian Ocean. Data corresponding to periods of rain fading were excluded from analysis. Statistics of signal-level variations were made for the period from July to September 1984 (Section III-B).

Darmstadt, Germany [8]: The Olympus satellite beacon signals at 12.50, 19.77, and 29.66 GHz were measured at the Research Institute of Deutsche Bundespost Telekom (currently known as the Research Centre of Deutsche Telekom AG) with two antennas of different sizes. The receiver outputs were sampled at a rate of 80 Hz, and averaged online over every second. Slowly varying signal contributions caused by attenuation due to gases, clouds, and rain were removed from the signal by a suitable hardware high-pass filter. Next, the signal variance was calculated over every minute from January 1990 to December 1992, with the exception of a few outage periods. Temperature and humidity were recorded as well, but only $N_{\rm wet}$ data from 1992 were evaluated, since earlier measured values showed a saturation effect for relative humidities $> 80\%$. Therefore, in this analysis, only the scintillation data from 1992 are used. The variances and the $N_{\rm wet}$ data were averaged over each month (Section III-A).

Eindhoven, The Netherlands [9]: The three Olympus beacons were received at Eindhoven University of Technology with one Cassegrain antenna with a frequency-dependent aperture efficiency. The signal was sampled at a rate of 3 Hz. The scintillation standard deviation was calculated over every minute in the period from January 1991 to May 1992, except from June to August 1991, when Olympus was out of order. Temperature and average humidity were also recorded over the same periods. The signal standard deviations and the calculated $N_{\rm wet}$ values were averaged over each month (Section III-A).

Fairbanks, AK [10]: Scintillation was measured in a propagation experiment using the 20.19 and 27.51 GHz beacons received from the ACTS satellite for the period December 1993 to November 1995. Beacon measurements were sampled at 1 Hz, a moving average over 120 s was subtracted from the signal, and the signal standard deviation over every hour was calculated. Dry conditions were identified using a sky temperature threshold. The standard deviations were averaged over the dry periods of each month. Meteorological parameters were also averaged over each month (Section IIIA). In addition, the cumulative statistics of signal level at 20.16 GHz are reported for the months February and August 1994. We added a small offset value to the statistics, to make the median value 0 dB (Section III-B).

Goonhilly, U.K. [6]: British Telecom carried out an experiment under contract to the INTELSAT organization to gather low-elevation data of tropospheric scintillation. The database, which was later analyzed in detail at Bradford University, Bradford, U.K., consisted of continuous 10 min standard deviations of signal strength at 11.20 GHz, radiometer temperature and meteorological parameters which were measured between February 1988 and August 1990. A "dry" data subset was extracted from the data, being characterized by a radiometer temperature < 80 K. The signal standard deviations and the meteorological data were averaged over each month (Section III-A). In addition [22], the signals received from November 1987 to October 1990 were analyzed. Difficulty was experienced in deriving fading and enhancement statistics with a signal that was fluctuating so significantly. The radiometer and ten minute averages of the beacon level were used extensively to establish a nominal clear sky level. The statistics were derived from simple addition of the total time each threshold was crossed, without any smoothing. The resulting distributions have been submitted to the databank "DBSG5" [13]. With this submission, it was mentioned that the fading data include rain effects as well. We added a small offset value to both statistics, to make the median value 0 dB (Section III-B).

Haystack, MA [1], [11]: Scintillation and meteorological parameters were measured during a one-year period. The seasonal averages of scintillation standard deviation at

7.3 GHz, temperature and relative humidity are reported (Section III-A).

Kirkkonummi, Finland [5]: Measurements were made of the beacons received from Olympus, from June 1992 to May 1993 at 19.77 GHz and from June to October 1992 at 29.66 GHz. The data were analyzed, under contract to ESA, at Helsinki University of Technology by the authors of this paper. The signal was sampled at 20 Hz and the variance was calculated over every minute. Data for which the rain intensity exceeded 0.03 mm/h were excluded from the analysis. $N_{\rm wet}$ was calculated from the temperature and humidity, which were measured at the site with a time resolution of one minute. Both the variances and the $N_{\rm wet}$ data were averaged over every month (Section III-A). In addition, the fade and enhancement distributions were derived over the same periods (Section III-B).

Leeheim, Germany [12]: The 11.79 GHz beacon of the orbital test satellite (OTS) was received by two different antennas at an experimental ground station of Deutsche Bundespost from June to December 1983. The postdetection bandwidth was 20 Hz; the signals were sampled at intervals of 72 ms and the one minute variances were calculated. Time periods with rain events leading to attenuations exceeding 0.4 dB were excluded. Meteorological measurements were also performed. The monthly averaged standard deviations and $N_{\rm wet}$ were submitted to the databank "DBSG5" [13]. Ortgies [14] found that thermal noise with a standard deviation of 0.0346 dB was present in the signal of the 3-m antenna. Therefore, we subtracted this contribution from the reported data for the 3-m antenna and a scaled contribution according to the Haddon/Vilar antenna averaging function for the 8.5-m antenna (Section III-A). In addition [14], a statistical analysis was made using the data received by the 3-m antenna from June 1 to September 13, 1983. The amplitude was sampled every two hours for six minutes. In total, 105 hours of data were evaluated. Time periods with rain events leading to attenuations exceeding 0.4 dB were excluded. Only a probability density distribution of signal level is reported, which we converted into a cumulative distribution of signal fade and enhancement. The long-term standard deviation is assumed to be the sum of the scintillation and thermal noise standard deviations, as reported by Ortgies (Section III-B).

Martlesham Heath, U.K. [15]: A four-year study of attenuation, depolarization, and scintillation on an INTELSAT-V satellite link was conducted by British Telecom Research Laboratories from June 1983 to May 1987 for INTELSAT. During the measured period, four different satellites served in succession, which were seen at elevation angles of 10.1°, 8.3°, 11.8°, and 10.1°, respectively, and operated at 11.45 and 11.20 GHz. Data were recorded each half second. A high-pass filter algorithm was used to separate the rapidly from the more slowly varying components of the measured attenuation signal. The data were divided into "event" data, characterized by mean fades $\geq$3 dB together with short pre- and post-event periods, and the remaining data. The standard deviation was calculated over every ten minutes block of data and averaged over each month for the "event" data set. No meteorological measurements are reported (Section III-A).

Ohita and **Okinawa, Japan** [1]: Measurements were made of an INTELSAT-V beacon during the year 1983, in the same project as the measurements at Yamaguchi (see hereafter). The signal standard deviations at 11.45 GHz as well as the temperature and relative humidity are reported, all averaged over each month (Section III-A).

Portsmouth, U.K. [23]: The 11.79 GHz beacon from the OTS was received at Portsmouth Polytechnic. For the scintillation analysis, the signal was high-pass filtered at 0.01 Hz, low-pass filtered at 28 Hz, and sampled at 3 Hz. A statistical analysis of signal level was made over a period of 725 h of data between June 20 and August 1, 1980. Since the signal fade and enhancement statistics were very similar, cumulative statistics are reported only for signal deviation, i.e., for fade and enhancement together. Therefore, here it will be assumed that fade and enhancement statistics were equal for this site (Section III-B).

Yamaguchi, Japan [16]: Long-term propagation experiments have been carried out using the INTELSAT-V satellite link at 11.45 GHz during the year 1983. Data were sampled at 1 Hz, and the standard deviations were calculated over every hour, and averaged over each month. Temperature, pressure, and humidity were observed four times a day at a nearby meteorological station. From these, the wet term of the refractivity at ground level $N_{\rm wet}$ was calculated and averaged over each month (Section III-A). In addition [1], the cumulative distributions of signal-level variations were obtained from measurements over the months of February, May, and August, 1983. These are the data upon which the Karasawa prediction model was based (Section III-B).

REFERENCES

[1] Y. Karasawa, M. Yamada, and J. E. Allnutt, "A new prediction method for tropospheric scintillation on earth-space paths," *IEEE Trans. Antennas Propagat.*, vol. 36, pp. 1608–1614, Nov. 1988.

[2] R. K. Crane and D. W. Blood, "Handbook for the estimation of microwave propagation effects," NASA Contract NAS5-25341, NASA GSFC Greenbelt, MA, Tech. Rep. 1, 7376-TR1, June 1979.

[3] ITU-R, "Propagation data and prediction methods required for the design of earth-space telecommunications systems," Recommendations ITU-R 5(F), Rec. PN 618-3, pp. 329–343, 1994.

[4] J. Haddon and E. Vilar, "Scattering Induced microwave scintillations from clear air and rain on earth space paths and the influence of antenna aperture," *IEEE Trans. Antennas Propagat.*, vol. AP-34, pp. 646–657, May 1986.

[5] M. M. J. L. van de Kamp, J. K. Tervonen, E. T. Salonen, and J. P. V. Poiares Baptista, "Scintillation prediction models compared to measurements on a time base of several days," *Electron. Lett.*, vol. 32, pp. 1074–1075, 1996.

[6] M. M. B. Mohd Yusoff, N. Sengupta, C. Alder, I. A. Glover, P. A. Watson, R. G. Howell, and D. L. Bryant, "Evidence for the presence of turbulent attenuation on low-elevation angle earth-space paths—Part I: Comparison of CCIR recommendation and scintillation observations on a 3.3° path," *IEEE Trans. Antennas Propagat.*, vol. 45, pp. 73–84, Jan. 1997.

[7] W. J. Vogel, G. W. Torrence, and J. E. Allnutt, "Scintillation fading on a low elevation angle satellite path: Assessing the Austin experiment at 11.2 GHz," in *8th Int. Conf. Antennas Propagat.*, Edinburgh, U.K., Apr. 1993, Inst. Elect. Eng. Conf. Pub. 370, vol. 1, pp. 48–51.

[8] G. Ortgies, "Prediction of slant-path amplitude scintillations from meteorological parameters," in *Proc. Int. Symp. Radio Propagat.*, Beijing, China, Aug. 1993, pp. 218–221.

[9] S. I. E. Touw, "Analyses of amplitude scintillations for the evaluation of the performance of open-loop ULPC systems," M.Sc. thesis, Eindhoven Univ. Technol., The Netherlands, 1994, pp. 129–134.
[10] C. E. Mayer, B. E. Jaeger, R. K. Crane, and X. Wang, "Ka-band scintillations: Measurements and model predictions," *Proc. IEEE*, vol. 85, pp. 936–945, June 1997.
[11] R. K. Crane, "Low elevation angle measurement limitations imposed by the troposphere: An analysis of scintillation observations made at Haystack and Millstone," MIT Lincoln Lab. Tech. Rep. 518, Lexington, MA, 1976.
[12] G. Ortgies and F. Rücker, "Diurnal and seasonal variations of OTS amplitude scintillations," *Electron. Lett.*, vol. 21, no. 4, pp. 143–145, 1985.
[13] ITU-R, "Acquisition, presentation and analysis of data in studies of tropospheric propagation," Recommendations ITU-R, vol. 5(A), Rec. PN 311-7, pp. 10–52, 1994.
[14] G. Ortgies, "Probability density function of amplitude scintillations," *Electron. Lett.*, vol. 21, no. 4, pp. 141–142, 1985.
[15] S. M. R. Jones, I. A. Glover, P. A. Watson, and R. G. Howell, "Evidence for the presence of turbulent attenuation on low-elevation angle earth-space paths—Part 2: Frequency scaling of scintillation intensity on a 10° path," *IEEE Trans. Antennas Propagat.*, vol. 45, pp. 85–92, Jan. 1997.
[16] Y. Karasawa, K. Yasukawa, and M. Yamada, "Tropospheric scintillation in the 11/14-GHz bands on earth-space paths with low elevation angles," *IEEE Trans. Antennas Propagat.*, vol. 36, pp. 563–569, Apr. 1988.
[17] J. K. Tervonen, M. M. J. L. van de Kamp, and E. T. Salonen, "Prediction model for the diurnal behavior of the tropospheric scintillation variance," *IEEE Trans. Antennas Propagat.*, vol. 46, pp. 1372–1378, Sept. 1998.
[18] E. Salonen and S. Uppala, "New prediction method of cloud attenuation," *Electron. Lett.*, vol. 27, no. 12, pp. 1106–1108, 1991.
[19] E. Salonen, S. Karhu, S. Uppala, and R. Hyvönen, "Study of improved propagation predictions," Helsinki Univ. Technol. Finnish Meteorolog. Inst., Final Rep. ESA/Estec Contract 9455/91/NL/LC(SC), pp. 83–87, 1994.
[20] C. J. Hahn, S. G. Warren, and J. London, "Edited synoptic cloud reports from ships and land stations over the globe, 1982–1991," NDP026B, Carbon Dioxide Inform. Anal. Ctr., Oak Ridge Nat. Lab., Oak Ridge, TN, 1996.
[21] O. P. Banjo and E. Vilar, "Measurement and modeling of amplitude scintillations on low-elevation earth-space paths and impact on communication systems," *IEEE Trans. Commun.*, vol. C-34, pp. 774–780, Aug. 1986.
[22] E. C. Johnston, D. L. Bryant, D. Maiti, and J. E. Allnutt, "Results of low elevation angle 11GHz satellite beacon measurements at Goonhilly," in *7th Int. Conf. Antennas Propagat.*, York, U.K., Apr. 1991, Inst. Elect. Eng. Conf. Pub. 333, vol. 1, pp. 366–369.
[23] T. J. Moulsley and E. Vilar, "Experimental and Theoretical statistics of microwave amplitude scintillations on satellite down-links," *IEEE Trans. Antennas Propagat.*, vol. 30, pp. 1099–1106, June 1982.
[24] M. M. J. L. van de Kamp, "Asymmetrical signal level distribution due to tropospheric scintillation," *Electron. Lett.*, vol. 34, no. 11, pp. 1145–1146, 1998.

Max M. J. L. van de Kamp (S'99) was born in Driebergen, The Netherlands, in 1963. He received the M.Sc. degree in electrical engineering from Eindhoven University of Technology (EUT), The Netherlands, in 1989.

He has been working as a Research Assistant in different research projects for the European Space Agency (ESA); he was at EUT from 1990 to 1994, at Helsinki University of Technology, Finland from 1995 to 1997, and in 1997 he returned to EUT. His main activities in these projects have been in satellite wave propagation research in the Olympus Propagation Experiment (OPEX).

Jouni K. Tervonen, for a photograph and biography, see p. 85 of the January 1999 issue of this TRANSACTIONS.

Erkki T. Salonen, for a photograph and biography, see p. 85 of the January 1999 issue of this TRANSACTIONS.

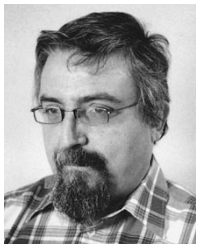

J. Pedro V. Poiares Baptista (M'93) was born in Beira, Mozambique. He received the Telecommunications Engineering degree from the University of OPorto, Portugal, in 1978, and the Laurea degree in electronic engineering from Politecnico of Milan, Italy, in 1983.

He is Senior Propagation Engineer at the European Space Research and Technology Centre of the European Space Agency, Noordwijk, The Netherlands, which he joined in 1986. Previously, he had worked at the University of Bradford, U.K., from 1984 to 1986, Politecnico of Milan, Italy, in 1979 and again from 1981 to 1983, and at Fondazione Ugo Bordoni, Rome, Italy, in 1980. Since 1978 he has worked in the modeling of propagation effects and on the development of atmospheric remote sensing retrieval algorithms.

Dr. Baptista is a member of the AGU.